Precision Measurement of the Proton Elastic Cross Section at High Q^2

W. Bertozzi, *S. Gilad (spokesperson)*, J. Huang,
B. Moffit (spokesperson)[†], P. Monaghan, N. Muangma, A. Puckett,
X. Zhan

Massachusetts Institute of Technology, Cambridge, MA, USA

A. Camsonne, J. P. Chen, E. Chudakov, C. W. de Jager, J. Gomez,
J.-O. Hansen, D. W. Higinbotham, M. Jones, J. LeRose, R. Michaels,
A. Saha, V. Sulkosky, *B. Wojtsekhowski (spokesperson)*

Thomas Jefferson National Accelerator Facility, Newport News, VA, USA

J. Arrington (spokesperson), D. F. Geesaman, K. Hafidi, R. Holt,
P. E. Reimer, P. Solvignon

Argonne National Laboratory, Argonne, Illinois, USA

A. Radyushkin

Old Dominion University, Norfolk, VA, USA
Thomas Jefferson National Accelerator Facility, Newport News, VA, USA

S. Abrahamyan, S. Mayilyan, A. Shahinyan

Yerevan Physics Institute, Yerevan, Armenia

D. Day, R. Lindgren, N. Liyanage, V. Nelyubin, B. E. Norum, K. Paschke

University of Virginia, Charlottesville, VA, USA

W. Boeglin, P. Markowitz, J. Reinhold

Florida International University, Miami, FL, USA

D. Armstrong, T. Averett, R. Feuerbach, M. Finn, L. Pentchev,
C. Perdrisat

College of William and Mary, Williamsburg, VA, USA

[†] contact person: Bryan Moffit (moffit@jlab.org)

J. Annand, D. Ireland, R. Kaiser, K. Livingston, I. MacGregor,
G. Rosner, B. Seitz

University of Glasgow, Glasgow, Scotland, UK

T. Holmstrom

Randolph-Macon College, Ashland, VA, USA

J. Calarco

University of New Hampshire, Durham, NH, USA

Y. Qiang

Duke University, Durham, NC, USA

G. Huber

University of Regina, Regina, Saskatchewan, Canada

K. A. Aniol, D. Margaziotis

California State University, Los Angeles, Los Angeles, California, USA

C. E. Hyde

Old Dominion University, Norfolk, VA, USA
Laboratoire de Physique Corpusculaire, Université Blaise Pascal, Aubière, France

B. Anderson, R. Subedi

Kent State University, Kent, OH, USA

and **The Hall A Collaboration**

Abstract

Using the base experimental equipment for Hall A, and beam energies of 6.6, 8.8, and 11 GeV, we propose to measure the proton elastic cross section to a statistical precision of better than 1% over a Q^2 range of 7–17.5 GeV^2. A few items of general purpose instrumentation are proposed to ensure that the total uncertainty will be below 2%. The resulting measurement will provide means for extracting the proton's magnetic form factor and be the benchmark for future cross section measurements at high Q^2. The experiment requests a total of 31 days for data taking, commissioning, and calibration. The experiment could be ready to run as soon as the high energy beam is available, and would be well suited to commissioning the upgraded beamline instrumentation for Hall A.

Contents

1 Collaboration Contributions to 12 GeV Baseline Equipment

There are four items listed under the Hall A 12 GeV baseline equipment:

- Arc energy measurement system
- the Compton polarimeter,
- the Moller polarimeter,
- the HRS readout electronics.

This collaboration intends to make major contributions to the readout electronics upgrade of HRS. In this project we plan to contribute in development of the software and hardware as well as in commissioning of electronics in beam. The members of the University of Virginia group are already involved in the present upgrade of the Compton polarimeter. As stated in previous 12 GeV PAC proposals, this involvement will continue into upgrading and commissioning of the Compton polarimeter for the high energy beam.

The collaboration intends to make major contributions in design and commissioning of the equipment for arc energy measurement system and the Moller polarimeter.

MIT will commit 1 FTE-year (1 postdoc and 1 graduate student) to the field measurements of the upgraded dipole magnets for use in the arc energy measurements.

In addition to the 12 GeV baseline equipment, this collaboration intends to make major contributions for the additional general purpose instrumentation and analysis techniques mentioned in this proposal. We note that these items may also be commissioned and used for the 6 GeV program. This collaboration has the expertise and resources to implement these proposed improvements.

2 Introduction

Nucleon electromagnetic form factors have provided significant information on the structure of the nucleon, been used to test predictions of pQCD, and provide one of the cornerstones of GPD modeling. Existing data at high Q^2 have large uncertainties (statistical and systematic), and also have large unknown uncertainties related to two-photon exchange (TPE) corrections and the contribution from G_E^p. This limits the ability to extract information on the Q^2 dependence, as well as introduction uncertainty in the knowledge of the elastic e–p cross sections at JLab kinematics. As the uncertainty on the e–p cross section yields a correlated uncertainty on measurements of G_E^p, G_M^n, and even G_E^n, as well as uncertainty in experiments that rely on a knowledge of the elastic cross section such as quasielastic A(e,e'p) measurements. The proposed measurements will provide both higher precision measurements of the cross section, and reduced dependence on uncertainties related to TPE and G_E^p.

The recent understanding of G_E^p/G_M^p indicates that the extraction of G_M^p from SLAC measurements has significant corrections that were not taken into account, and which modify both the overall size and Q^2 dependence of G_M^p. While future understanding of the high Q^2 behavior of G_E^p/G_M^p and two-photon exchange can be used to improve extraction from the SLAC data, the proposed measurements has three main advantages over the existing SLAC data. First, we will significantly improve the statistical and systematic uncertainties on the cross section measurements. Second, because the measurement is at lower ϵ, the contributions from G_E^p are significantly smaller than for the large Q^2 SLAC data (where G_E^p may be negative and large). Third, while there is still significant uncertainty in the two-photon exchange corrections at large Q^2, this contributes to the uncertainty in extracting G_M^p, but does not increase the uncertainty in determining the e–p elastic cross section values needed by other high-Q^2 measurements at JLab. The SLAC data, taken at significantly higher beam energies, would have to be extrapolated down to lower ϵ values to be used as input for JLab measurements, and this extrapolation would be affected by the uncertainty in the two-photon exchange corrections. We will be measuring the cross sections at kinematics where any TPE corrections will be very similar to what is seen in other experiments at JLab.

2.1 Physics Overview

2.2 Overview

In view of the remarks in the Introduction, we consider several interesting issues that motivate us to explore further the measurement of $e - p$ elastic cross section at JLab:

(1) While the form factor deviates significantly from the dipole fit, it is not clear to what extend it is consistent (or inconsistent) with pQCD scaling.

(2) What is the power of the Q^2 dependence as a function of momentum, and how does the form factor approach the pQCD limit?

(3) What information can be learned about the GPDs constrained by new precision measurements of the cross section?

(4) Is it possible to distinguish the VDM mechanism from direct coupling of the virtual photon to a single quark?

In order to present a framework for addressing these issues, we next present discussions of reaction mechanisms in the pQCD and GPD approaches.

2.3   pQCD Mechanism

The traditional framework for the interpretation of hard exclusive reactions has been perturbative QCD (pQCD) [1]. This is based in part on the observation that the onset of scaling in Deep Inelastic Scattering (DIS) occurs at the relative low scale of $Q^2 \sim 1 - 2$ GeV^2, thereby giving rise to expectations that pQCD might also be applicable to the exclusive processes in the range of a few GeV^2. In the pQCD approach to the FFs, the three valence quarks are active participants in the hard subprocess, which is mediated by the exchange of two hard gluons. The soft physics is contained in the so-called valence quark distribution amplitudes. The pQCD mechanism leads naturally to the so-called constituent counting rules for exclusive processes.

Indeed, the observation that many exclusive reactions, such as elastic electron scattering, pion photoproduction, and RCS, approximately obey scaling laws has led some to believe that the pQCD mechanism dominates at experimentally accessible energies. There seems to be little theoretical disagreement that the pQCD mechanism dominates at sufficiently high energies; however, there is no consensus on how high is "sufficiently high." Indeed, despite the observed scaling, absolute cross sections calculated using the pQCD framework are very often low compared to existing experimental data, sometimes by more than an order of magnitude. Moreover, several recent JLab experiments that measure polarization observables also disagree with the predictions of pQCD. In the G_E^p experiments [2, 3] the slow falloff of the Pauli form factor $F_2(Q^2)$ up to Q^2 of 5.6 GeV^2 provides direct evidence that hadron helicity is not conserved, contrary to predictions of pQCD. This has been interpreted in terms of logarithmic corrections to the leading order pQCD behavior, coming from angular momentum of the quarks [4]. However, reproducing the lower Q^2 data where polarization measurements of G_E^p/G_M^p exist requires an unreasonably large value of Λ_{QCD} [5]. Measurements of G_E^p at higher Q^2, combined with the higher precision measurements of G_M^p proposed here, will allow for a more detailed examination of the logarithmic corrections, as well as providing a consistency check on these corrections.

Similar findings were made in the π^0 photoproduction experiment [6], where both the non-zero transverse and normal components of polarization of the recoil proton are indicative of hadron helicity-flip, which is again contrary to the predictions of pQCD.

2.4 Handbag Mechanism

The handbag mechanism offers new possibilities for the interpretation of hard exclusive reactions. For example, it provides the framework for the interpretation of so-called deep exclusive reactions, which are reactions initiated by a high-Q^2 virtual photon. The soft physics is contained in the wave function describing how the active quark couples to the proton. This coupling is described in terms of GPDs. The GPDs have been the subject of intense experimental and theoretical activity in recent years [7, 8]. They represent "super-structures" of the proton, from which are derived other measurable structure functions, such as parton distribution functions (PDF) and form factors.

The nucleon form factors and the PDFs extracted from DIS are the only quantities where one can directly probe specific values of the GPDs. They provide the cornerstones when modeling GPDs, and the only constraints at high Q^2, and make it easier to interpret the results of other measurements that are sensitive to moments of GPDs, or combinations of GPDs. Having reliable knowledge of the GPDs in the regions where this is possible is important in maximizing what we can learn from the broader program of GPD studies.

2.5 Additional Remarks

It is important to realize that the issues posed at the start of this section are not limited to the elastic $e - p$ reaction. Indeed, they are questions that need to be addressed by all studies of the proton using exclusive reactions in the hard scattering regime. The old paradigm for addressing these questions was the pQCD mechanism and the distribution amplitudes. It is quite likely that the new paradigm will be the handbag mechanism and GPDs. In any case, the reaction mechanism needs to be tested, not only over a wide range of kinematic variables but also over a wide range of different reactions. Elastic electron scattering at high momentum transfer offers the best possibility to test the mechanism free of complications from additional hadrons.

2.6 Summary of Physics Goals

We propose measurements of the electron scattering from the proton at an incident electron energy of 6.6, 8.8 and 11 GeV, at large scattering angles corresponding to Q^2 range 7 -17.5 GeV^2. The specific physics goals are as follows:

(1) Provide a stringent test of the notion that the elastic F$_1$ form factor exhibit pQCD like scaling behavior at Q^2 above 7-8 GeV^2.
(2) Determine the form factor G_M^p with accuracy several times higher that it is known from existing single data set obtained at SLAC.

(3) Measure the cross section of $e - p$ scattering at kinematics used in JLab experiment to allow accurate normalization for study of G_M^n and many others.

The overall precision with which we will address these physics goals will be discussed in section 3.

2.7 Background - Previous Measurements

Measurement of the proton's elastic electromagnetic form factors has been of considerable interest to the Jefferson Lab experimental program and is critical for describing the proton's underlying structure.

In terms of the Sachs electromagnetic form factors, the differential cross section for elastic ep scattering is written compactly as

$$\frac{d\sigma}{d\Omega} = \sigma_{\mathrm{mott}} \frac{\epsilon (G_E^p)^2 + \tau (G_M^p)^2}{\epsilon (1 + \tau)}, \tag{1}$$

where the structure-less cross section σ_{mott} is given by

$$\sigma_{\mathrm{mott}} = \left(\frac{\alpha}{2E} \frac{\cos \frac{\theta}{2}}{\sin^2 \frac{\theta}{2}} \right)^2 \frac{E'}{E}, \tag{2}$$

with $\tau = Q^2/4M_p^2$, and $\epsilon = [1 + 2(1 + \tau)\tan^2(\theta/2)]^{-1}$.

These form factors have been extracted in Rosenbluth Separation experiments via elastic scattering using either traditional inclusive $p(e, e')p$ measurements [9–14], or elastic $p(e, p)e'$ [15]. In addition, polarization transfer measurements [3, 16] have dramatically improved the extraction of G_E^p at large Q^2.

These recent polarization transfer measurements have generated much excitement in the nuclear physics community, showing a large discrepancy in the measurement of the ratio of the electric form factor to the magnetic form factor, G_E^p/G_M^p, compared to that measured by the other methods. The current explanation of this discrepancy is the application of radiative corrections at leading order to extract the ratio. These corrections can vary significantly with ϵ. Of considerable interest at present has been the inclusion of the full two-photon exchange contributions to these corrections. A few reviews of the current understanding from an experimental and theoretical point of view are found in Ref. [5, 17–19].
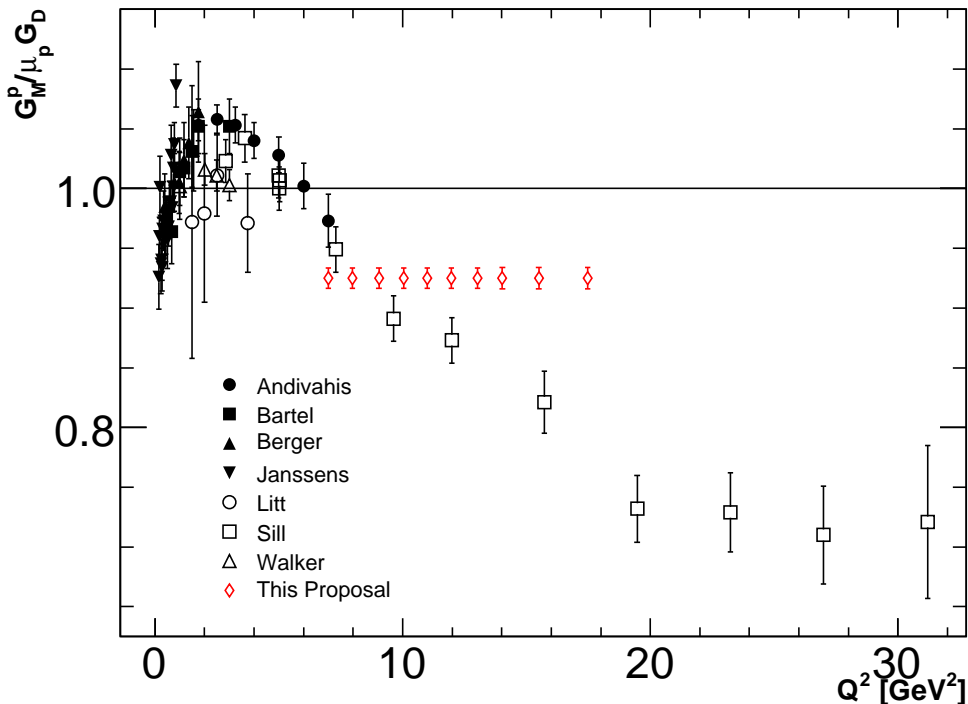
Fig. 1. Published world data for $G_M^p/\mu_p G_D$ as a function of Q^2 (Refs. [9–14, 20]). Uncertainties shown do not include the effect of the normalization uncertainty, which is 3% on the Sill et al. cross sections, and projected to be 1–1.2% for the proposed measurements.

2.8 *Motivation for the Current Proposal*

As shown in Figure 1, a majority of the Q^2 coverage for G_M^p is for $Q^2 < 8$ GeV^2. The best data above 8 GeV^2 is the Sill et al., measurement from SLAC [20]. The cross section uncertainties on the Sill measurement vary from 4% at $Q^2 = 5$ GeV^2, to 8% for $Q^2 \approx 20$ GeV^2, not including an overall normalization uncertainty of 3%. An earlier measurement [21] also measured elastic scattering in this Q^2 range, but had much larger uncertainties (5–30%, with a normalization uncertainty of approx. 5%).

The extraction of G_M^p from this data was performed assuming scaling, i.e. $G_E^p = G_M^p/\mu_p$. This assumption had G_E^p contribute 6% (2%) to the cross section at $Q^2 = 5$ GeV^2 (20 GeV^2). From the recent polarization transfer measurements, we now know that the contribution from G_E^p is significantly less for the Q^2 values where G_E^p/G_M^p has been measured. The true contribution from G_E^p will be zero near $Q^2 \approx 6$–7 GeV^2, increase as Q^2 increases, where G_E^p/G_M^p becomes negative and increases in magnitude with Q^2. If the linear behavior seen in the polarization measurements [3] continues, $|\mu_p G_E^p/G_M^p|$ will become greater than one above $Q^2 \approx 13$ GeV^2, and the contribution from G_E^p will actually be *larger* than was assumed in the previous analyses. Thus, instead of the contribution from G_E^p decreasing by 4% between Q^2 of 5 and 15–20 GeV^2, it will *increase* by 4%, yielding a

10

noticeably modified Q^2 dependence for G_M^p.

In addition, two-photon exchange (TPE) effects also yield a correction to the extracted value of G_M^p. Except for the IR-divergent terms, these contributions were completely neglected in the analysis of all previous measurements. Therefore, while the cross sections are measured at the 5–10% level, the uncertainty in G_M^p is larger than was assumed in previous extractions, and difficult to determine.

Future measurements of G_E^p/G_M^p at large Q^2 can be used to improve the extraction of G_M^p from the SLAC data, and help correct for the artificial Q^2 dependence introduced by the assumption of form factor scaling. However, the uncertainties on the high Q^2 SLAC data are fairly large, and the contributions from G_E^p will be significant, because the measurements are all at large ϵ. For example the contribution from G_E^p, assuming the linear behavior observed in polarization transfer measurements continues, would imply a 4% correction to the cross section data around 18 GeV^2, while for the measurements proposed here and taken at lower ϵ values, the contribution would be only 1–2%. While the 12 GeV upgrade will extend direct measurements of G_E^p/G_M^p to higher Q^2, we will only have direct measurements over some of the Q^2 range, and the reduced sensitivity to G_E^p will allow for a cleaner extraction of G_M^p.

The uncertainty in the two-photon exchange corrections at these high Q^2 yield an additional uncertainty in the extraction of G_M^p. These corrections are somewhat larger for the measurements proposed here than for the SLAC measurements. However, for the SLAC measurements, the TPE corrections also make it difficult to reliably extrapolate the SLAC cross section measurements to the JLab kinematics since they were taken at higher beam energy and thus lower ϵ. As discussed below, the elastic e–p cross section is an important input to several other experiments, and so even with the larger TPE corrections, it is more reliable to use the measurements proposed here, at similar energies to other future JLab measurements, than to try and extrapolate the SLAC cross section measurements.

The measurements proposed here will allow for better extractions of both the proton's magnetic form factor and the elastic e–p cross section. In addition, it will provide better constraints on the high-Q^2 behavior of the form factors, and thus allow for stronger tests of models of the nucleon form factor. This will be of particular importance as other JLab measurements improve the Q^2 coverage of the other electromagnetic form factors. These measurements will also provide the highest Q^2 constraints on Generalized Parton Distributions (GPDs) from exclusive reactions. Only the DIS measurements of the parton distribution functions can provide information on the GPDs at higher Q^2 values, and the Q^2 dependence of these is well understood.

Figure 2 shows the precision with which we can test the prediction of a $1/Q^4$ behavior for G_M^p. The red points are the power as taken by comparing pairs of G_M^p measurements from Sill [20]. To have a reasonable measure of the Q^2 dependence, one needs to look at the data over a large Q^2 range. The solid red line shows the power taken from using all of the Sill data, and the dashed lines show the uncertainty, if we assume that there is no change
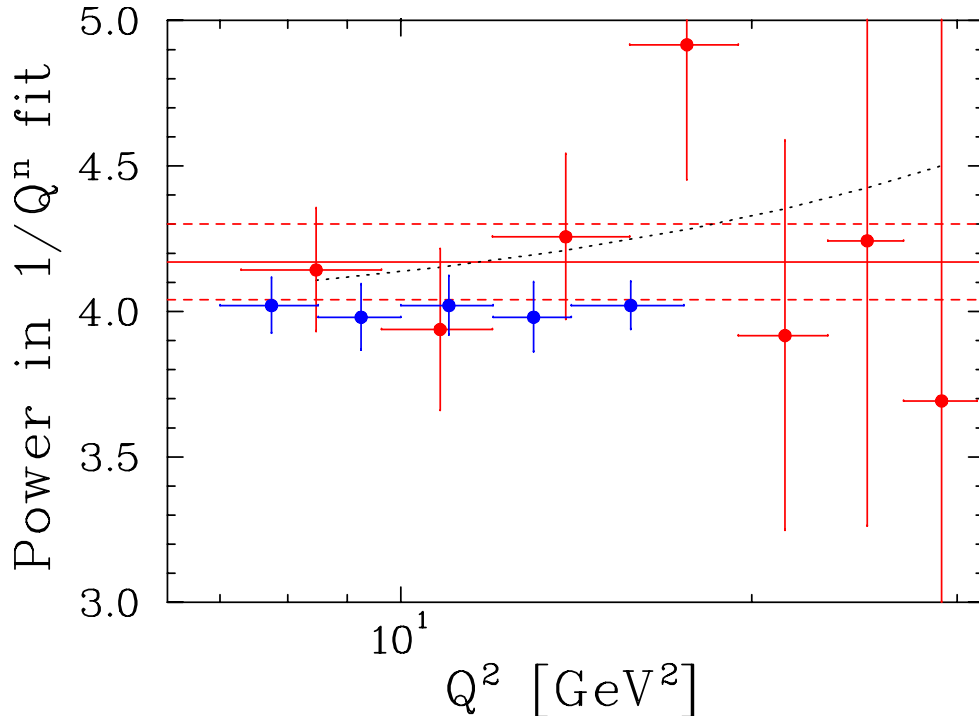
Fig. 2. The power, n, on a $1/Q^n$ fit to individual pairs of G_M^p points. The red points are from the SLAC data, while the blue points are for the proposed measurements (offset to show the Q^2 separation of the points). The curves are described in the text.

in the falloff of the form factor as we go to higher Q^2. If we try to look for a change in this behavior with Q^2, e.g. by fitting these extractions to a straight line, we obtain the black dotted line. Clearly, we cannot use these data to study the approach to scaling, or to make a precision determiniation of the Q^2 dependence except by integrating over the entire Q^2 range. The blue points show what can be done with the proposed measurements, using every other point (i.e. a typical spacing of 2 GeV^2 for each extraction). As you can see, each point does a better job of determining the power of the Q^2 falloff better than the combined result from all of the Sill data above 7 GeV^2, allowing both a better measure, and a measure of the approach to the expected perturbative behavior.

In addition to studying G_M^p by itself, these data will provide precision measurements on the elastic e–p cross section. All of the other electromagnetic form factor measurements are taken relative to either G_M^p or the elastic e–p cross section. Polarization transfer measurements in e–p scattering provide only the ratio of G_E^p/G_M^p, and one needs the cross section to obtain the absolute values for the individual form factors. Measurements of G_M^n rely on either the ratio of neutron to proton QE scattering on the deuteron ($D(e,e'n)/D(e,e'p)$) or the asymmetry in scattering from polarized Helium-3. In both cases, one is measuring the ratio of the elastic e–n cross section to the elastic e–p cross section, and so the uncertainty in σ_{e-p} translates into an error on σ_{e-n} and thus G_M^n and G_E^n, which is again measured as a ratio to G_M^n. Thus, the error in the $e-p$ elastic cross section can yield a significant and highly correlated error in all of the electromagnetic form factors. Such a correlated error in all of the measurements could be an important limiting factor in using

12

these measurements to constrain models of the nucleon structure.

The best previous cross section measurements in this range have uncertainties at the 5–10% level. In addition, because these are taken at smaller scattering angles (and higher energies), the extrapolation to JLab kinematics for the same Q^2 values also relies on our knowledge of G_E^p and TPE at these very large Q^2 values. Therefore there will be additional poorly known uncertainties in the value, and possibly the Q^2 dependence, of the cross section. This will translate into uncertainties of all of the nucleon electromagnetic form factors, as well as other high Q^2 measurements of elastic or quasielastic scattering.

To achieve these goals, we propose the measurement of the proton's elastic cross section from a range in Q^2 from 7–17.5 GeV^2 using the existing High Resolution Spectrometers of Hall A. With a relatively short amount of time (31 days) and a few additional pieces of general purpose instrumentation a high precision would be obtained. Thus creating a precision benchmark for high Q^2 cross section measurements for future experiments. As the contribution of G_E^p to the cross section is expected to be negligible for much of this Q^2 range, and small for all Q^2 values, this measurement will provide a precise determination of the evolution of G_M^p at high Q^2.

The proposed measurements will improve the precision on the cross section measurements from 5–10% down to below 2%. Because they are measured at kinematics appropriate for other JLab 12 GeV measurements, there will be minimal additional theoretical uncertainty in extrapolating to the kinematics of other JLab measurements. In addition, these measurements will be at smaller ϵ values than the SLAC measurements, yielding smaller corrections from G_E^p, even at the largest Q^2 values where they may well be *larger* than assumed in the analysis where form factor scaling was assumed. We also include two Q^2 points that will be measured at each of two different beam energies. This will not be used to perform a Rosenbluth separation, but will provide measurements of G_M^p at three different epsilon values to test the corrections due to G_E^p and two-photon exchange. The point at lower ϵ will have an extremely small contribution from G_E^p, even if G_E^p is quite large, but somewhat larger TPE corrections. The higher ϵ point will be somewhat more sensitive to the value of G_E^p, but have a significantly smaller TPE correction.

2.9 Factors Contributing to Accuracy of the Experimental Results

A measurement of the elastic cross section to this precision is quite an undertaking, as systematic factors must be understood to an unprecedented level. We plan to aggressively reduce the uncertainties in these factors that contribute to the accuracy of the experimental results:

- Incident beam energy and it's stability,
- Electron scattering angles and the mapping of the spectrometer focal plane variables to the target variables,
- Spectrometer acceptance with an extended target,

- Target density the stability of the luminosity under experimental conditions.
- Radiative corrections.

Our plan to address these factors, include the following:

- Absolute determination of the beam energy with the eP method and upgraded arc. Beam energy stability monitored with Tiefenback energy,
- Construction and commissioning of the Precision Angle Measurement (PAM) device and installation of an additional VDC in each spectrometer focal plane,
- Utilization of the PAM micro-strip detector (MSD) that will be made to be slightly larger than and placed in front of the spectrometer collimator. Several solid carbon targets with 1-2 cm spacings along the incident beam direction for measure of the acceptance as a function of the target length,
- Use of the Hall A luminosity monitor to measure the frequency spectrum of target density fluctuations and monitor the stability of the experimental luminosity throughout the entire run.
- Standard radiative corrections (not including TPE) are well know and are understood to the 0.5% level. TPE corrections have gone through a great deal of progress a should be better know by the time of the running of the experiment. A few kinematic points are also proposed to measure the ϵ dependence of the elastic cross section, which has been shown to be correlated with the TPE corrections.

These items will be explained in more detail in the following sections.

3 Proposed Experiment

We propose to measure the proton elastic cross section and use these data to extract G_M^p over the Q^2 range of 7–17.5 GeV^2. At beam energies of 6.6 GeV, 8.8 GeV, and 11 GeV, both Hall A High Resolution spectrometers (HRSs) will be primarily in a symmetric configuration in electron detector mode to double the counting statistics and provide a means for additional systematic checks. The technical details of the HRSs can be found in Ref. [22]. A beam current of 80 μA combined with a 20 cm target with a density of 4.3×10^{22} protons/cm^3 (0.072 g/cm^3) provides a luminosity of about 4.3×10^{38} cm^{-2}s^{-1} allowing the proton elastic cross section to be measured in only 31 days (including all commissioning and overhead).

We begin this section by showing the specific kinematics for this measurement, followed by a detailed description of the experimental setup. Finally, we provide a summary of the requested beam time to complete the measurement.

3.1 Detailed Kinematics for the Measurement

E_e (GeV)	Q^2 (GeV)^2	θ_e (deg)	E' (GeV)	ϵ	Rate (Hz)	Time (hours)	Events
6.6	7.0	35.4	2.869	0.62	7.45	0.7	40k
6.6	8.0	42.0	2.351	0.51	2.29	2.4	40k
6.6	9.0	52.0	1.782	0.37	0.48	11.6	40k
6.6	10.0	67.0	1.249	0.23	0.15	38.3	40k
8.8	9.0	29.3	4.000*	0.67	3.38	3.3	40k
8.8	10.0	33.3	3.465*	0.59	1.31	8.5	40k
8.8	11.0	38.0	2.945	0.51	0.53	10.5	40k
8.8	12.0	44.0	2.423	0.41	0.21	26.7	40k
8.8	13.0	53.0	1.859	0.30	0.06	67.4	28k
11.0	13.0	31.3	4.065*	0.58	0.36	21.2	28k
11.0	14.0	35.0	3.525*	0.50	0.17	39.0	24k
11.0	15.5	42.0	2.742	0.39	0.05	52.8	20k
11.0	17.5	58.0	1.689	0.21	0.01	271.4	16k
						517.8	

Table 1

Kinematics for the proposed measurement. Calculated rates assume a luminosity of 4.3×10^{38} cm^{-2}s^{-1}, solid angle coverage of 5.4 msr, and proton form factor parametrization from Ref. [23]. Kinematics with scattered electron energy (E') with an asterisk (*) indicate measurements that will only be done with the Left HRS. The total time is slightly less than the sum of the individual times because the Right HRS will take data on the higher Q^2 points for the kinematics where only the Left arm can reach the required momentum.

The kinematics for the proposed experiment are shown in Table 1. Each Q^2 point has been optimized to achieve a statistical precision in the proton elastic cross section of 0.5-0.8%. Three Q^2 points at 9, 10 and 13 GeV^2 are repeated to check for systematics arising

from the change in beam energy from 6.6 GeV to 8.8 GeV and 8.8 GeV to 11 GeV. The ϵ dependence to the cross section is expected to be weak at this high Q^2 (due to $\tau(G_M^p)^2/\epsilon(G_E^p)^2 \simeq 35$). Four Q^2 points involve scattered electron energies (E') that are beyond the current capabilities of the Right HRS. Therefore, these points will measured using only the Left HRS.

3.2 Experimental Setup

3.2.1 The Targets

We plan to use the standard Hall A cryogenic target ladder, composed of a liquid hydrogen target and Carbon and Aluminum solid targets for optics calibrations and background determinations. We plan to use the 20 cm LH$_2$ racetrack cells that feature vertical cryogenic fluid flow to reduce the effects of target density fluctuations. These target cells have been successfully used in previous high luminosity Hall A experiments. Background from quasielastic scattering from the aluminum windows will be evaluated with aluminum foils used to simulate the contribution. The optics targets (with 1-2 cm spacing along $z_{\rm lab}$) will be used to optimize the spectrometer matrix elements using an improved method similar to the one current used and outlined in Ref. [24]. This method is discussed in a later section. We will also take some runs at the lower Q^2 values on a 4cm hydrogen target, as a test of the normalization and target length acceptance corrections.

3.2.2 The Spectrometer setup

The proposed measurement will use both High Resolution Spectrometers (HRSs) in electron detection mode. Each detector package, shown in Figure 3 will consist of:

- A set of three Vertical Drift Chambers (VDC) for tracking.
- A pair of trigger scintillator planes (S0 and S2m).
- Gas Cherenkov counter for pion rejection and trigger.
- A lead glass calorimeter for addition pion rejection and trigger.

We plan to augment the pair of VDCs, currently present in each spectrometer arm, with an additional and identical VDC to reduce systematics of track reconstruction efficiency. Hall A currently has a spare VDC readily available, and the components and electronics required to build a second chamber is on-site. To have them installed, the first scintillator trigger plane (S1) will need to be removed. The S0 scintillator plane will be installed to provide high trigger efficiency.

The main trigger, to cleanly select electron events, will be the coincidence signal between the Gas Cherenkov and S2m scintillator plane. Singles from S2m, as well as a set of random pulsers (generated from a small scintillator in a black box with a radioactive source), will serve as auxiliary triggers to check the efficiency of the main trigger. The
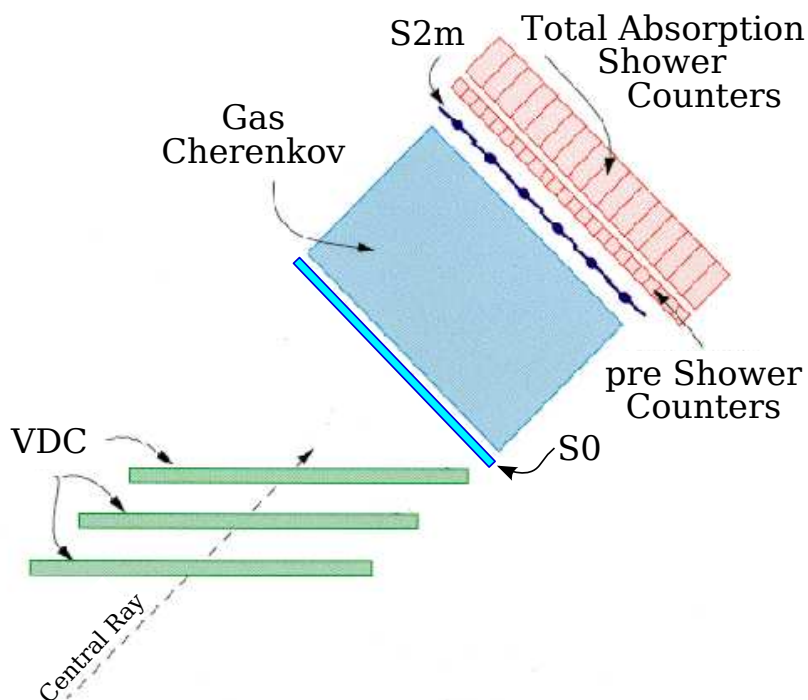
Fig. 3. Schematic of detector package for the HRSs.

lead glass calorimeter (pre-shower and shower detectors) signals will serve as a powerful instrument for background suppression. Two secondary triggers, the coincidence of S0 and the Gas Cherenkov, and the coincidence of S0 and S2m, will also be used. This will allow for continuous measurement of the S2m and Cherenkov trigger efficiencies.

3.2.3 Beam Energy Measurement

To measure the incident beam energy, this experiment will use the upgraded Arc method and eP systems. These methods have shown the capability of providing a precision of $\leq 3 \times 10^{-4}$ [22] and show good agreement with each other. Both methods will require upgrade to be used after the 12 GeV upgrade [25]. The eP system will require a minor upgrade to its electron trigger to allow it to function at larger beam energies.

The beam energy spread will be monitored constantly using the Synchrotron Light Interferometer (SLI) that was commissioned and used during E94-107 (showing that the accelerator was able to achieve a beam energy spread as small as 6×10^{-5} (FWHM) [26]). We plan to use the OTR and the Tiefenback Energy as a cross check to monitor the beam energy stability.

3.2.4 Beam Intensity and Luminosity Monitoring

The beam intensity will be monitored using the two RF cavity monitors located just upstream of the raster, along with the newer cavity monitors (that also measure position) that are located just upstream of the target. This original system has worked successfully for 10 years, and provides a measure of the beam current to $\leq 0.5\%$ [22]. To accurately normalize the elastic cross section, a beam calibration will need to be performed and we plan to include the signal from the cavity monitors for each event in the data acquisition (along with the normal scaler readout system).

Monitoring of the stability of the target density will be provided by the Hall A luminosity monitor. This system also provides the capability of determining the frequency spectrum of density fluctuations induced by local beam heating. A scaler-based, integrating data acquisition system will be constructed to allow for the detector signals from this monitor to be inserted into the data stream allowing for the constant monitoring of the target density over the entire run.

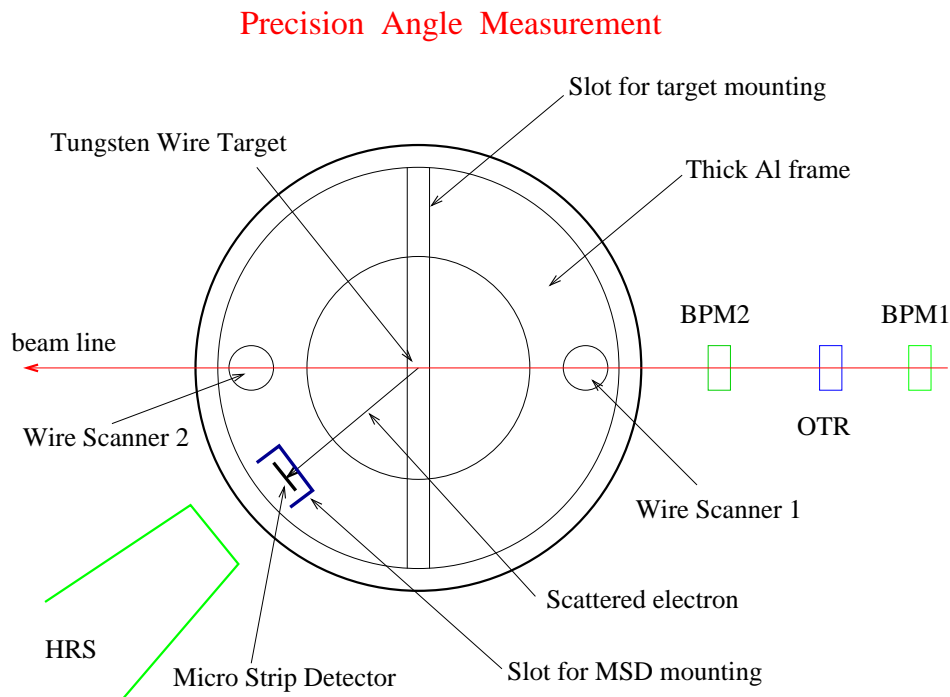### 3.2.5 Incoming beam and scattering angle

Fig. 4. Schematic of Precision Angle Measurement (PAM) device as presented in Ref. [27]. Note that only one MSD and Spectrometer are pictured, where this proposed experiment will require the use of two of each.

Apart from the strip line beam position monitors, just upstream of the target location, a *Precision Angle Measurement (PAM)* device will allow for improved accuracy and greater reliability in determining the incoming beam angle as well as the electron scattering angle.

A rough schematic of PAM is shown in Figure 4, as it was presented in [27]. The main features of this devices include:

- Two wire scanners to monitor the beam position up and downstream of the target,
- A vertically installed 10 μm tungsten wire target to define the center of the target ladder,
- A silicon micro-strip detector (MSD) in front of each spectrometer (slightly larger than the acceptance defining collimator) to detect scattered charged particles before they enter the spectrometer. These MSDs will be of the same design as that shown in Figure 5.

All of these are mounted on to a aluminum frame. Slots for the MSD, within the frame, will allow for the movement of the MSD for variety spectrometer angles. The original design incorporated the entire frame within the scattering chamber, but may be easily adapted for use outside of the chamber.
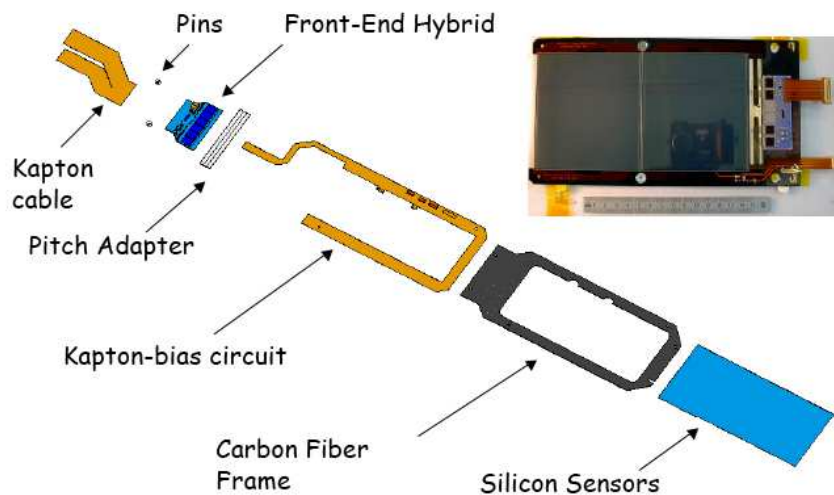

Fig. 5. Schematic and picture of the micro-strip detector (MSD) designed for the CMS experiment at the LHC. The intermediate electronic board design is currently being discussed for JLab use.

With the tungsten wire target and MSD installed, the scattering angle would be measured by the spectrometer and MSD to the level of 0.05 mrad (or better). This measurement would also serve to measure the acceptance and optical properties of the spectrometer. Measurement of the incoming beam angle will be measured by the wire scanners which can then be used to calibrate the cavity and stripline beam position monitors just upstream of the target. In addition, PAM will allow for improved optics studies of the spectrometer, improving our knowledge of the optics and acceptance, and thus allowing for a better absolute uncertainty in the cross section measurements.

The simplicity of the design of this apparatus, is such that it may be designed and commissioned for experiments requiring precision angle measurements before the 12 GeV energy upgrade.

3.3 Requested Beam Time

To complete the precision measurement of the proton elastic cross section for a range in Q^2 of 7–17.5 GeV^2, we request 31 days. Table 2 provides a breakdown of how this time is allocated.

Item	Hours
Production on LH$_2$	518
Background from Aluminum Foils	91
Optics calibrations and angle measurements (PAM)	80
eP and Arc Energy Measurements	12
Target density measurements/tests	8
Data on 4cm LH$_2$ targets	8
BCM calibration	8
Beam energy changes	8
Checkout/calibration	12
Total	**745**

Table 2
Detailed beam time request.

A large fraction of the beam time requested is for production data taking at the highest Q^2 point (17.5 GeV^2). We note that this data may also be taken with a single spectrometer in parallel (or parasitically) to the running of the 12 GeV Polarization Transfer experiment (proposed for this PAC) [28] if it is also approved.

4 Systematic Uncertainties

We plan to be aggressive in minimizing the systematic uncertainties so that the statistical precision of the proposed measurement is not undermined. It is our assertion that this goal is realized by the inclusion of a small amount of general purpose items to the Hall A baseline equipment, and improved analysis techniques. In this section, we discuss the systematics that are expected to contribute to the point to point and normalization uncertainties.

4.1 Incident Energy

Calibration of the absolute energy will be done using the eP and Arc method. At present, these methods provide an absolute precision of $(3\text{–}4){\times}10^{-4}$. Stability of the beam energy central value can be monitored based on the BPMs in the Hall A arc, and both the absolute energy and energy drifts can be verified using the elastic peak position. Assuming that the eP precision is still $(3\text{–}4){\times}10^{-4}$ for the higher energy beams, the resulting uncertainty on the cross-section measure is below $\pm0.3\%$ for all kinematics.

4.2 Scattering Angle

Measurement of the central scattering angle of the spectrometers is typically be provided by direct survey and usually provides a precision of better than ±0.2 mrad. This yields a cross section uncertainty of less than 0.3%. However, on several occassions a discrepancy has been found to be up to several mrad [29]. Without another independent measurement, this error would not have been found. For this reason, a separate absolute angle measurement must be made by some version of the PAM device. With this device, discussed in the previous section, we expect to better the precision of the measurement to be improved by at least a factor of two, and to provide a more reliable measurement of the spectrometer pointing.

4.3 Incident Beam Angle

The incident beam angle is currently determined utilizing the stripline Beam Position Monitors (BPMs) that are calibrated to provide an absolute position of the beam through use of wire scanners (superharps). The current implementation of this method provides an uncertainty of 0.1 mrad [22]. This corresponds to an uncertainty contribution of less than $\pm0.2\%$ in the cross section, which can be further reduced using the PAM device.

4.4   Beam Charge

With careful monitoring and calibration of the beam current monitors, the beam charge is typically to known to ±0.5% or better, as long as the beam current is large enough that uncertainties in the BCM offsets for zero current are not small. This is typically only an issue for currents below 10 μA. For the proposed measurements, we will run at 80 μA, and will have a fixed beam current for all of the main data taking. Under these circumstances, the uncertainty is largely in the absolute normalization, and the drifts over time are smaller [15]. We assume a 0.3% point-to-point normalization, and a 0.4% scale uncertainty.

4.5   Target Density

The 20 cm racetrack cells have provided Hall A with reduced density fluctuations compared to the cigar-shaped cells (whose performance is detailed in Refs. [30, 31]). Although there is no current detailed literature showing the racetrack cell performance, we make an educated guess that they are equivalent or better than the tuna-can shaped cells (which also feature a vertical cryogenic flow). These cells were shown to contribute a 0.5% systematic error to previous measurements. We plan to perform a detailed study of the density fluctuations from the racetrack cell before or during the commissioning of this experiment. The standard procedure to characterize beam-related target density fluctuations is to take data as a function of beam current, and compare the normalized yield as a function of beam current. We will take beam current scans for both high rate and low rate kinematics, to ensure that we do not mistake density fluctuations for deadtime, efficiency, multiple track corrections, or other rate-dependent effects. We will also take beam current scans on a solid target, to provide a calibration for the case with no density fluctuations. This has allowed for precise measurements of the current-dependent density fluctuations, which are small and very nearly linear with current for the transverse flow target designs.

4.6   Radiative Corrections

The radiative corrections are significant at these Q^2 values, and the approximations sometimes used at lower energies begin to be less reliable. The prescriptions used for elastic scattering have been studied in this Q^2 range [32, 33], and the standard radiative corrections, shown in Figure 6 (a-d), (not including two-photon exchange) are understood at the 0.5% level.

Most previous experiments quoted uncertainties that were dominated by two-photon exchange (TPE) corrections (shown in Figure 6 (e,f)), where were assumed to be at the 1-1.5% level. In fact, it now appears that these corrections may be at the several percent level and are at this time still quite uncertain at these kinematics. There is a great deal
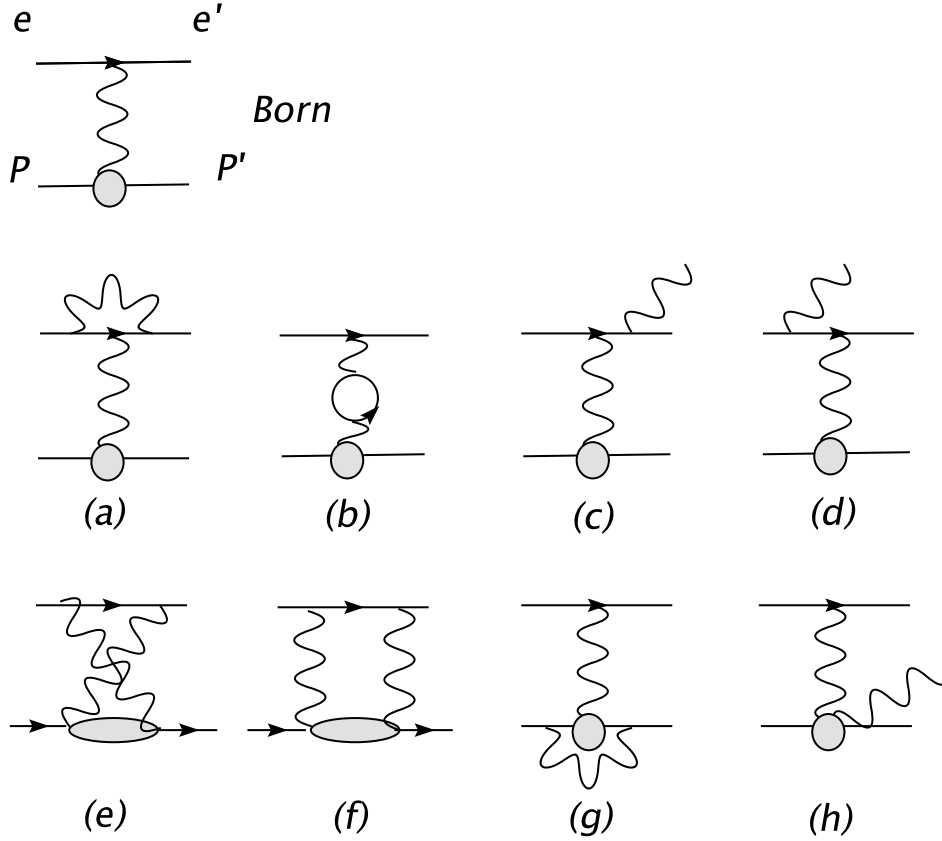
Fig. 6. Feynman diagrams for Born Approximation and radiative corrections (a-h) for electron-proton scattering.

of progress on the calculation of these corrections, and several experiments underway to help extract TPE in order to verify the calculations. We have three kinematics where we extract G_M^p at multiple ϵ values, which will also provide a test of the calculated TPE corrections (when combined with future measurements of G_E^p).

However, in many cases, the TPE uncertainties are not relevant. For other measurements made at the same Q^2 and beam energy, the TPE corrections are identical, and the uncertainty involved in separating G_M^p from TPE corrections does not affect the uncertainty in the total cross section. So experiments such as the measurement of the neutron magnetic form factor, which measures the ratio of e–n to e–p elastic cross sections, and quasielastic scattering measurement at high Q^2 simply need the e–p cross section, and are not affected by the uncertainty in TPE. Therefore, we *do not* include an uncertainty from TPE in the extracted cross sections, although it will yield an additional uncertainty in the extraction of G_M^p. Given our present understanding of TPE corrections, this would yield an uncertainty of ~2% on the extraction of G_M^p, based on a rough estimate of the model-dependence of current calculations [33, 34]. This will of course be reduced as our understanding of the TPE corrections improves.

.

23

The current procedures used to determine the spectrometer acceptance typically results in a systematic error in the cross section of about 2%. The uncertainty is smaller for elastic scattering, because the elastic peak populates only the central region of the momentum acceptance, and because one integrates over the peak, making the result less sensitive to the accuracy of the momentum reconstruction.

The largest issues are the loss of events at apertures within that magnetic elements, and the target length acceptance. We will perform careful studies of the optics and acceptance of the spectrometer, taking data with optics target, thin foils spaced 1-2 cm apart, using both sieve slits and using the PAM device to determine the angles of the events. In addition, we will use a collimator that is slightly narrower, approximately 5.4 cm compared to the standard 6.3 cm opening. With this collimator, far fewer events are lost inside the spectrometer magnets (mainly on the sides of the dipole), making the target length acceptance much flatter, and easier to model. We will take measurements on a 4 cm cell for some of the lower Q^2 settings at a few different angles, to verify the normalization of the acceptance corrections for the longer targets. With careful modeling of the spectrometer, the uncertainty in the acceptance of the spectrometer (for elastic scattering from a 4cm cell) can be known to 1% [35]. With the careful optics studies and additional information provided by the PAM, we hope to do this well or better for the extended targets.
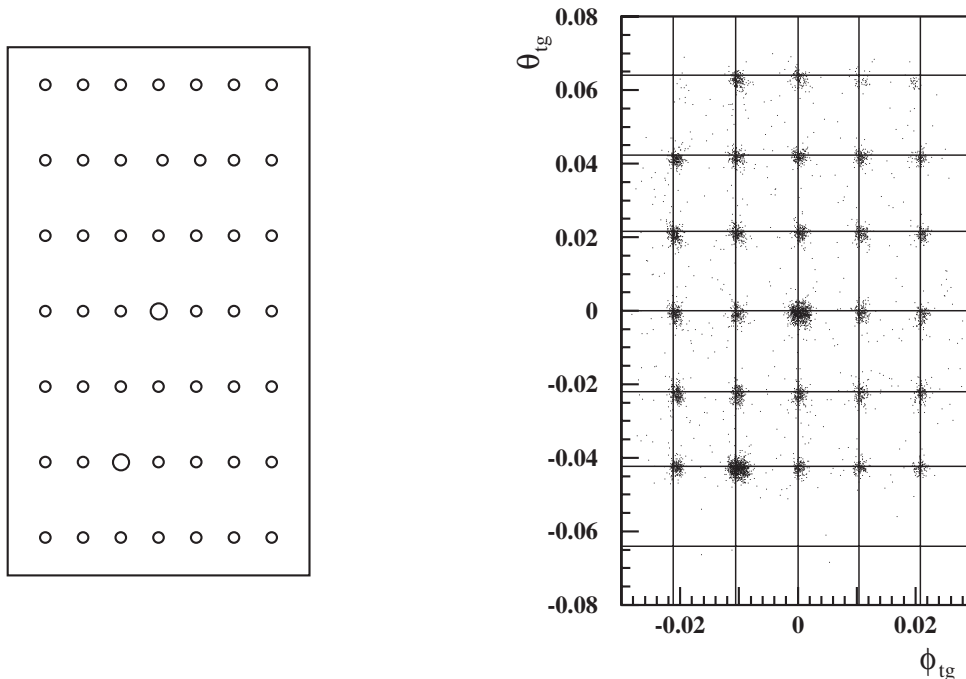

Fig. 7. Schematic of a sieve slit (left) and reconstructed events to the target in-plane and out--of-plane angles (right) as presented in Ref. [22]. Horizontal and vertical lines in the right plot, indicate the predicted locations of the reconstructed holes.

We also intend to improve the current optics optimization analysis code that was first

developed based on a χ^2-minimization of scattered events through a sieve-slit placed at the entrance to the spectrometer, shown in Figure 7. This analysis has proven to work well using low beam energy on a carbon foil where tight cuts in reconstructed δ are made on the elastic peak to help remove sieve punch through events. This analysis is more difficult at larger beam energy and scattering angle due to the fall of the ^{12}C elastic cross section. In this case, quasi-elastic scattering from ^{12}C can be used but does not cleanly remove punch-through events. This leads to a background distribution, that is not necessarily flat, that causes systematic shifts of the reconstructed sieve pattern from the χ^2-minimization routine.

To improve this analysis method at high beam energies a set of routines to perform a "peak"-search will be included. This procedure would entail finding maximum peak heights in focal plane distributions and locating their cooresponding peaks in the sieve plane. The χ^2-minimization technique would then use this information in conjunction with using the typical cuts on events that appear to be within the vicinity of a sieve hole (which are subject to non-uniform background distributions).

4.8 Detector Efficiencies and CPU/Electronic Dead Time

Detector efficiencies for the HRS are generally high with relatively small uncertainties. Because our rates are always low, corrections due to multiple tracks and electronic dead time, which tend to be more difficult to correct precisely, should be very small. The third VDC installed in each arm will also serve to reduce the systematics associated with the track reconstruction efficiency. Computer dead time should also be very small, although this correction is well understood even for high rates. We will have multiple triggers, to allow for constant monitoring of the detector efficiencies. This should allow us to achieve an overall uncertainty to the cross section to about $\pm 0.5\%$, which we take to be roughly equal parts point-to-point and scale contributions.

4.9 Endcap Subtraction

Dummy target runs will be taken to measure the contribution from the Aluminum endcaps of the cryotarget. The contribution from the endcaps will be approximately 5% or less, and the main uncertainty in the subtraction comes from knowing the relative Aluminum thicknesses of the target walls and the dummy target (which we plan to measure by means of X-ray attenuation to the 1% level), and the difference in radiative corrections for the real target and the dummy. We will be able to verify the normalization by comparing data in the superelastic region for all settings. The uncertainty in the endcap subtraction should be known to a few percent of the size of the subtraction, or about 0.1-0.2%. We assume a 0.1% scale, and 0.1% point-to-point uncertainty.

4.10 π^- Background

The π^- rates within the spectrometer acceptance have been calculated based on fits to SLAC data [36]. This calculation is the same as that typically used for inclusive π^- photonproduction and is understood to be accurate to within a factor of two. We estimate the ratio of π^-/e rates to be in the range of 2–200 within the δ region of interest (integrating from the elastic peak to the pion threshold) for the proposed kinematic points. This result is quite acceptable given the online (using the Gas Cherenkov as a trigger) and offline analysis (using the lead glass calorimeters) pion rejection factor that is typically obtained in Hall A of at least 10^4 with an electron detection efficiency of 99.5% [37].

4.11 Total Systematic Uncertainty

Contributions to the uncertainty are summarized in Table 3.

Source	$\Delta\sigma/\sigma$ (%)
Point to point uncertainties	
Incident Energy	<0.3
Scattering Angle	0.1–0.3
Incident Beam Angle	0.1–0.2
Radiative Corrections*	0.3
Beam Charge	0.3
Target Density Fluctuations	0.2
Spectrometer Acceptance	0.4–0.8
Endcap Subtraction	0.1
Detector efficiencies and dead time	0.3
Sum in quadrature	*0.8–1.1*
Normalization uncertainties	
Beam Charge	0.4
Target Thickness/Density	0.5
Radiative Corrections*	0.4
Spectrometer Acceptance	0.6–1.0
Endcap Subtraction	0.1
Detector efficiencies and dead time	0.4
Sum in quadrature	*1.0–1.3*
Statistics	*0.5–0.8*
Total (Scale+Rand.+Stat.)	**1.2–1.7**

* Not including TPE; see subsection 4.6

Table 3
Expected systematic uncertainties in $d\sigma/d\Omega$. The lower numbers indicate the values we hope to achieve if the new PAM device functions as well as desired.

5 Summary

In conclusion, we proposed to measure the proton elastic cross section in the Q^2 range of 7–17.5 GeV^2 to a statistical precision of less than 1%. Understanding of systematic contribution will be aided by a few additional general purpose instrumentation for the baseline Hall A equipment and the improvement of the current analysis techniques. Measurements of form factors whose analysis requires an accurate proton cross section will greatly benefit from the precision of this measurement. Also, extraction of G_M^p from this measurement will provide a means for accurate determination of G_E^p from future polarization transfer measurements.

We request **31 days** to successfully complete the experiment.

References

[1] S. J. Brodsky and G. P. Lepage, "Helicity Selection Rules and Tests of Gluon Spin in Exclusive QCD Processes," *Phys. Rev.* **D24** (1981) 2848.

[2] **Jefferson Lab Hall A** Collaboration, M. K. Jones *et al.*, "G_E^p/G_M^p ratio by polarization transfer in $\vec{e}p \rightarrow e\,\vec{p}$," *Phys. Rev. Lett.* **84** (2000) 1398–1402, `nucl-ex/9910005`.

[3] **Jefferson Lab Hall A** Collaboration, O. Gayou *et al.*, "Measurement of G_E^p/G_M^p in $\vec{e}p \rightarrow e\,\vec{p}$ to $Q^2 = 5.6$ GeV^2," *Phys. Rev. Lett.* **88** (2002) 092301, `nucl-ex/0111010`.

[4] A. V. Belitsky, X.-d. Ji, and F. Yuan, "A perturbative QCD analysis of the nucleon's Pauli form factor F2(Q**2)," *Phys. Rev. Lett.* **91** (2003) 092003, `hep-ph/0212351`.

[5] J. Arrington, C. D. Roberts, and J. M. Zanotti, "Nucleon electromagnetic form factors," `nucl-th/0611050`.

[6] K. Wijesooriya *et al.*, "Polarization measurements in neutral pion photoproduction," *Phys. Rev.* **C66** (2002) 034614.

[7] X. Ji, "Deeply virtual Compton scattering," *Phys. Rev. D* **55** (Jun, 1997) 7114–7125.

[8] A. V. Radyushkin, "Scaling Limit of Deeply Virtual Compton Scattering," *Phys. Lett.* **B380** (1996) 417–425, `hep-ph/9604317`.

[9] L. Andivahis *et al.*, "Measurements of the electric and magnetic form-factors of the proton from $Q^2 = 1.75$ (GeV/c)^2 to 8.83 (GeV/c)^2," *Phys. Rev.* **D50** (1994) 5491–5517.

[10] W. Bartel *et al.*, "Measurement of proton and neutron electromagnetic form-factors at squared four momentum transfers up to 3 (GeV/c)^2," *Nucl. Phys.* **B58** (1973) 429–475.

[11] C. Berger, V. Burkert, G. Knop, B. Langenbeck, and K. Rith, "Electromagnetic form-factors of the proton at squared four momentum transfers between 10 fm^{-2} and 50 fm^{-2}," *Phys. Lett.* **B35** (1971) 87.

[12] T. Janssens, R. Hofstadter, E. B. Hughes, and M. R. Yearian, "Proton form factors from elastic electron-proton scattering," *Phys. Rev.* **142** (1966) 922–931.

[13] J. Litt *et al.*, "Measurement of the ratio of the proton form-factors, G(E) / G(M), at high momentum transfers and the question of scaling," *Phys. Lett.* **B31** (1970) 40–44.

[14] R. C. Walker *et al.*, "Measurements of the proton elastic form-factors for 1 (GeV/c)$^2 \leq Q^2 \leq 3$ (GeV/c)^2 at SLAC," *Phys. Rev.* **D49** (1994) 5671–5689.

[15] I. A. Qattan *et al.*, "Precision Rosenbluth measurement of the proton elastic form factors," *Phys. Rev. Lett.* **94** (2005) 142301, `nucl-ex/0410010`.

[16] V. Punjabi *et al.*, "Proton elastic form factor ratios to $Q^2 = 3.5$ GeV^2 by polarization transfer," *Phys. Rev.* **C71** (2005) 055202.

[17] H.-y. Gao, "Nucleon electromagnetic form factors," *Int. J. Mod. Phys.* **E12** (2003) 1–40, `nucl-ex/0301002`.

[18] C. E. Hyde-Wright and K. de Jager, "Electromagnetic Form Factors of the Nucleon and Compton Scattering," *Ann. Rev. Nucl. Part. Sci.* **54** (2004) 217–267, `nucl-ex/0507001`.

[19] C. F. Perdrisat, V. Punjabi, and M. Vanderhaeghen, "Nucleon electromagnetic form factors," `hep-ph/0612014`.

[20] A. F. Sill *et al.*, "Measurements of elastic electron - proton scattering at large momentum transfer," *Phys. Rev.* **D48** (1993) 29–55.

[21] D. H. Coward *et al.*, "Electron - Proton Elastic Scattering at High Momentum Transfers," *Phys. Rev. Lett.* **20** (1968) 292–295.

[22] J. Alcorn *et al.*, "Basic Instrumentation for Hall A at Jefferson Lab," *Nucl. Instrum. Meth.* **A522** (2004) 294–346.

[23] J. J. Kelly, "Simple parametrization of nucleon form factors," *Phys. Rev.* **C70** (2004) 068202.

[24] N. Liyanage, "Optics Calibration of the Hall A High Resolution Spectrometers using the new C++ Optimizer," 2002. Jefferson Lab TN 02-012.

[25] J. Arrington *et al.*, "Hall A 12 GeV Upgrade – Pre-Conceptual Design Report," 2005. http://hallaweb.jlab.org/12GeV/cdr/cdr.ps.

[26] M. Iodice *et al.*, "High Resolution Spectroscopy of $^{12}_\Lambda$B by Electroproduction," `arXiv:0705.3332`. [nucl-ex].

[27] B. Wojtsekhowski, "An Instrument for Precision Angle Measurement," 2001. Jefferson Lab TN 01-046.

[28] C. F. Perdrisat, L. Pentchev, E. Cisbani, V. Punjabi, and B. Wojtsekhowski, "Large Acceptance Proton Form Factor Ratio Measurements at 13 and 15 GeV^2 Using Recoil Polarization Method," 2007. Jefferson Lab 12 GeV PAC32 Proposal.

[29] R. Feuerbach. private communication.

[30] D. Armstrong, B. Moffit, and R. Suleiman, "Target Density Fluctuations and Bulk Boiling in the Hall A Cryotarget," 2003. Jefferson Lab TN 03-017.

[31] P. Ulmer, "LH2 Target Density in Hall A Experiment E01-020," 2005. Jefferson Lab TN 05-064.

[32] R. Ent *et al.*, "Radiative corrections for (e,e'p) reactions at GeV energies," *Phys. Rev.* **C64** (2001) 054610.

[33] A. Afanasev. private communication.

[34] A. V. Afanasev, S. J. Brodsky, C. E. Carlson, Y.-C. Chen, and M. Vanderhaeghen, "The two-photon exchange contribution to elastic electron nucleon scattering at large momentum transfer," *Phys. Rev.* **D72** (2005) 013008, `hep-ph/0502013`.

[35] **E94110** Collaboration, M. E. Christy *et al.*, "Measurements of electron proton elastic cross sections for 0.4 (GeV/c)^2 < Q^2 < 5.5 (GeV/c)^2," *Phys. Rev.* **C70** (2004) 015206, `nucl-ex/0401030`.

[36] D. E. Wiser. PhD thesis, University of Wisconsin, 1977. (unpublished).

[37] A. Ketikyan, H. Voskanyan, and B. Wojtsekhowski, "About Shower Detector Software," 1997. http://www.jlab.org/∼armen/sh_web_page/software/espdoc.ps.